Article citation info:
Kurzydym D. 1D model of a three-way catalyst in MATLAB/Simulink for assessing pollutant reduction in the NEDC emission test. Combustion Engines. 2026;206(3):159-169. https://doi.org/10.19206/CE-218134

Damian KURZYDYM

Combustion Engines
Polish Scientific Society of Combustion Engines

1D model of a three-way catalyst in MATLAB/Simulink for assessing pollutant reduction in the NEDC emission test

ARTICLE INFO

Received: 30 November 2025
Revised: 8 February 2026
Accepted: 14 February 2026
Available online: 20 February 2026

A one-dimensional model of a three-way catalyst (TWC) was developed in MATLAB/Simulink, consisting of a monolith pressure-drop module and a reaction block for CO/HC/NO_x. The model was validated against a reference GT-SUITE solution, with agreement in levels and trends. Kinetic parameters were tuned and verified using emission tests in the NEDC cycle. The model reproduces pressure drop, instantaneous profiles, and cumulative emissions upstream and downstream of the catalyst. Satisfactory agreement between predicted reductions and NEDC measurements confirms the model's suitability for assessing TWC effectiveness and for calibration under test conditions. The approach is computationally lightweight and ready to be extended to other driving cycles, additional physical effects, and exhaust aftertreatment systems such as a GPF.

Key words: *three-way catalyst (TWC), 1D modeling, pressure drop, reaction kinetics, emission reduction*

1. Introduction to the three-way catalyst

The development of effective three-way catalysts is crucial for mitigating harmful automotive emissions, specifically targeting nitrogen oxides, carbon monoxide, and unburnt hydrocarbons [7]. These catalysts achieve this by facilitating oxidation of carbon monoxide and hydrocarbons, alongside the reduction of nitrogen oxides. These converters are mainly used in gasoline engines that operate close to the ideal air-fuel ratio. They rely on noble metals such as platinum, palladium, and rhodium embedded in a washcoat to enable highly efficient pollutant conversion [1]. However, even with these advancements, automobiles remain significant contributors to HC, CO, and NO_x emissions, with a substantial portion occurring during cold start operations [6]. Advanced modeling techniques are required to precisely predict catalyst light-off and breakthrough across diverse driving conditions, including accelerations, decelerations, and high-speed extra-urban phases [14]. To avoid the high costs associated with extensive experimental optimization, computational simulations have become an invaluable tool in catalyst development and performance assessment [1, 16]. Consequently, a robust one-dimensional (1D) model capable of simulating the complex transient behavior of catalytic converters, offers a computationally efficient alternative for optimizing catalyst design and control strategies [13, 17].

A typical three-way catalytic converter (Fig. 1) comprises a ceramic or metallic monolith substrate with numerous parallel channels, coated with a washcoat containing precious metals (e.g., Pt, Pd, Rh) and oxygen storage materials (e.g., ceria) [1, 7]. This complex structure is vital for providing a large surface area for chemical reactions and improving catalytic efficiency by enabling easier adsorption and reaction of exhaust gases. The catalytic reactions, which convert pollutants such as carbon monoxide, hydrocarbons, and nitrogen oxides into less harmful substances such as carbon dioxide, water, and nitrogen, are governed by complex kinetic mechanisms influenced by these material properties and dynamic operating conditions [6, 9]. The interaction between the exhaust gas and the catalyst surface, particularly within the washcoat, involves complex mass transfer phenomena and detailed chemical kinetics, which significantly influence overall conversion efficiency [6, 20].

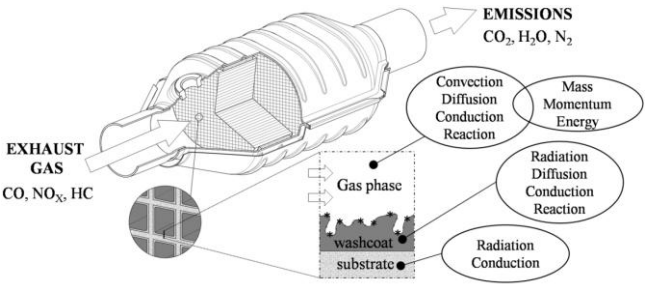

Fig. 1. Catalytic converter with physical and chemical processes [10]

To accurately capture these phenomena, various mathematical models have been developed, with one-dimensional models offering a balance between computational efficiency and predictive accuracy for simulating automotive catalytic converter performance, especially under transient conditions [4, 16]. These 1D models typically approximate the entire monolith by analyzing a single representative channel, then extrapolating the results using geometric scaling parameters like cell density, wall thickness, and monolith dimensions [13]. The development of advanced 1D models for exhaust aftertreatment systems is crucial for a comprehensive simulation of engine and catalyst setups. Studies demonstrate that integrated 1D models can effectively predict the impact of aftertreatment systems on performance, ensuring high accuracy while maintaining acceptable computational time. Such an approach enables the optimization of catalyst geometry and pollution conversion efficiency [8].

The novelty of this work is the development of an original 1D three-way catalyst model built from scratch in MATLAB/Simulink. The model integrates pressure-drop prediction with chemical reaction kinetics and is capable of

simulating both steady-state and transient operating conditions. Its applicability is demonstrated through full-cycle emission assessment under the New European Driving Cycle (NEDC), providing a lightweight, flexible analysis tool.

2. Research methodology

2.1. 1D equations describing pressure drop

Accurate prediction of this pressure drop is crucial for optimizing exhaust system design, as an uneven flow distribution can degrade conversion efficiency and accelerate catalyst aging [5]. Darcy-Weisbach or Darcy-Forchheimer equations, often employed for calculating pressure drop in pipe flows, can be adapted for monolith channels by considering factors such as friction losses and changes in momentum due to flow acceleration or deceleration [11, 13]. However, it is important to note that the pressure drop within the monolithic brick itself is a primary contributor to the overall pressure drop in the catalytic converter, with the inlet and outlet cones also playing a significant role in flow distribution. Therefore, a detailed understanding of the fluid dynamics, including turbulence and momentum transfer within the wash-coated channels, is essential for precise pressure drop modeling. Additionally, viscous and inertial effects, alongside turbulence, significantly influence the pressure drop within the monolith, which can vary considerably with temperature. This necessitates the application of porous media models to accurately represent the complex flow resistance, where the monolith is treated as a distributed resistance with empirically derived coefficients to account for inertial and viscous losses [5, 10].

The three-way catalyst (TWC) was modeled as a regular monolith, where the channel pitch p (center-to-center distance between adjacent channels) was determined based on the cell density (cpsi). The total frontal area A_{face} was set equal to the converter face area.

$$A_{face} = \pi \left(\frac{D}{2}\right)^2 \tag{1}$$

$$p = \frac{1}{\sqrt{cpsi}} \tag{2}$$

where: A_{face} – monolith frontal area, m^2, D – substrate diameter, m, p – channel pitch, m, cpsi – cell density, cells/in^2 (converted to cells/m^2).

Square-channel geometry is characterized by the open channel width derived from pitch and wall thickness, the hydraulic diameter is taken equal to this width, and from these, the monolith's open frontal area and total open flow area are obtained.

$$a = p - t = D_h \tag{3}$$

$$OFA = \left(\frac{a}{p}\right)^2 \tag{4}$$

$$A_{open} = OFA \cdot A_{face} \tag{5}$$

where: a – channel width, m, t – channel wall thickness, m, D_h – hydraulic diameter of a single channel (equals a for a square), m, OFA – open frontal area fraction, A_{open} – total open area for flow, m^2.

Density is evaluated from the ideal-gas law using the inlet pressure and temperature for air. Dynamic viscosity follows the Sutherland correlation (for air), providing a realistic temperature dependence. This air-based closure is lightweight and sufficiently accurate for the pressure-drop calculations used here.

$$\rho = \frac{p_{in}}{R_{spec} \cdot T_{in}} \tag{6}$$

$$\mu(T_{in}) = \mu_0 \left(\frac{T_{in}}{T_0}\right)^{3/2} \frac{T_0 + C}{T_{in} + C} \tag{7}$$

where: ρ – gas density, kg·m^{-3}, p_{in} – absolute inlet pressure to the substrate, Pa, T_{in} – gas temperature at catalyst inlet, K, R_{spec} – specific gas constant (287), J·kg^{-1}·K^{-1}, μ(T) – dynamic viscosity, Pa·s, Sutherland constants (air): μ_0 = $1.716 \cdot 10^{-5}$, Pa·s, T_0 = 273.15 K, C = 111 K.

The bulk velocity through the channels is obtained from mass flow and the total open area.

$$U = \frac{\dot{m}}{\rho \cdot A_{open}} \tag{8}$$

where: U – mean channel (superficial) velocity, m·s^{-1}, ṁ – total mass flow rate, kg·s^{-1}.

The pressure loss across the TWC monolith is modeled as the sum of a viscous term consistent with Darcy–Weisbach and an inertial (minor-loss) term [5]. The effective coefficients A and B are determined empirically from calibration and together account for entrance and exit penalties and washcoat effects, with different values for coated and uncoated substrates.

$$\Delta p_{TWC} = A \frac{\mu U L}{D_h} + B \frac{\rho U^2}{2} \tag{9}$$

where: Δp_{TWC} – monolith pressure drop, Pa, L – substrate length, m, A – viscous loss coefficient (calibrated), B – inertial loss coefficient (calibrated). Coated monolith: A = 32, B = 0.50. Uncoated monolith: A = 28.4, B = 0.41.

Table 1 summarizes the input data used for the 1D catalyst pressure-drop simulation and the corresponding geometric parameters.

Table 1. Input data for the 1D TWC pressure drop model

Simulation time [s]	100
Temperature [K]	300
Mass flow rate [kg/s]	linear ramp (0.01 → 0.22)
Working medium	air
Tested catalyst	
Diameter [m]	0.1057 (4.16 in)
Length [m]	0.0754 (2.97 in)
Channel density [m^{-2}]	6.2×10^5 (400 cpsi)
Wall thickness [m]	1.65×10^{-4} (0.165 mm)
Active layer (washcoat)	No

2.2. 1D equations describing the reaction kinetics

A thorough understanding of the kinetics governing the catalytic reactions is crucial for accurately modeling the performance of three-way catalysts, as these reactions are highly sensitive to temperature, gas composition, and the

presence of inhibiting species. These kinetic parameters, often determined through experimental methods, are then incorporated into the model to predict conversion efficiencies for CO, HC, and NO_x under varying operating conditions [16]. Although one-dimensional models neglect radial gradients within channels, they adequately describe thermo and fluid dynamic behavior, as validated through comparisons with two-dimensional models [19]. This simplification significantly reduces the computational complexity compared to full 3D models, which would be impractical for transient regulatory cycle simulations due to extensive effort and slow computational times [4]. Such 1D models treat all channels of the monolith identically, assuming uniform boundary conditions, which allows for efficient simulation without sacrificing significant accuracy for many engineering applications [15]. However, most of these models are 1D plug-flow models that couple separate conservation equations for the gas and solid phases using transport coefficients [7]. In an efficient three-way catalyst, the primary reactions involve oxidation of CO and hydrocarbons to CO_2 and H_2O, and reduction of NO to N_2 and CO_2 [14]. The selection of appropriate kinetic expressions, such as Langmuir-Hinshelwood type rate equations, is critical for accurately representing the reaction rates and their dependence on various species concentrations and temperatures [18].

For the purpose of developing a 1D TWC catalyst model with detailed reaction mechanisms, the gas composition at the catalyst inlet was taken from a GT-SUITE ready-made example. The total molar concentration C_t is computed from inlet pressure and temperature by the ideal-gas law [16], and the initial species concentrations follow as $C_i^{(0)}$. These values define the initial condition for the 1D plug-flow calculation.

$$C_t = \frac{p_{in}}{R_u \cdot T_{in}} \tag{10}$$

$$C_i^{(0)} = y_i \cdot C_t \tag{11}$$

where: C_t – total molar concentration of the gas mixture at reactor inlet, mol·m^{-3}, R_u – universal (molar) gas constant (8.314), J·mol^{-1}·K^{-1}, $C_i^{(0)}$ – inlet molar concentration of species i, mol·m^{-3}, y_i – inlet mole fraction of species i.

To keep the 1D model compact, chemically similar species are grouped into pseudo-components with effective properties. Hydrocarbons (HC) are treated as a C3 lump that combines propane (C_3H_8) and propylene (C_3H_6), with effective oxygen demand and effective molar mass consistent with the GT-SUITE reference setup. Nitrogen oxides are handled as an NO_x lump formed by pooling nitric oxide (NO) and nitrogen dioxide (NO_2), and the lump is expressed using nitric oxide as the reference for kinetics and mass calculations. This approach preserves the key effects on oxygen consumption and product formation (CO_2 and H_2O) while reducing computational cost and the number of calibrated parameters.

$$y_{HC} = y_{C_3H_6} + y_{C_3H_8} \tag{12}$$

$$y_{NOx} = y_{NO} + y_{NO_2} \tag{13}$$

A plug–flow, isothermal 1D catalyst channel is mapped from axial coordinate x to a residence-time coordinate using the bulk gas velocity U:

$$t = \frac{x}{U} \tag{14}$$

$$\frac{dC_i}{dt} = R_i(\mathbf{C}, T) \tag{15}$$

where: t – residence-time coordinate, s, x – axial coordinate, m, C_i – molar concentration of species i, mol·m^{-3}, $R_i(\mathbf{C}, T)$ – volumetric reaction rate for species i evaluated at the current state $(\mathbf{C}, T)$, mol·m^{-3}·s^{-1}, $\mathbf{C}$ – vector of all species concentrations, mol·m^{-3}, T – as temperature, K.

For a monolith of length L the total residence time is:

$$\tau = \frac{L}{U} \tag{16}$$

where: τ – total residence time, s.

The reactor is split into N_{seg} axial segments and the marching step in the residence-time domain is

$$\Delta t = \frac{\tau}{N_{seg}} \tag{17}$$

where: N_{seg} – no. axial segments, Δt – marching step, s.

With an explicit Euler update (i.e., a first-order forward time integration that evaluates the reaction rate at the current state and advances by Δt), each species is updated segment-by-segment as:

$$C_i^{k+1} = C_i^k + R_i\left(\mathbf{C}^k, T\right)\Delta t \tag{18}$$

where: $k = 0, \ldots, N_{seg} - 1$.

This axial "time-marching" is equivalent to an upwind discretization of the 1D plug-flow balance, neglecting axial dispersion. The explicit scheme is stable for sufficiently small Δt. In the simulations, stability is ensured by choosing N_{seg} such that Δt remains small across the temperature window.

The catalytic chemistry is represented by three global reactions for CO oxidation, NO reduction by CO, and lumped C3 hydrocarbon oxidation. Kinetics follow an Arrhenius temperature law with power-law dependencies on reactant concentrations. Reaction orders and stoichiometric oxygen demand for the HC lump are effective (lumped) parameters calibrated to GT-SUITE data.

$$CO + \frac{1}{2}O_2 \rightarrow CO_2 \tag{19}$$

$$2CO + 2NO \rightarrow 2CO_2 + N_2 \tag{20}$$

$$C_3H_x + \nu_{O2,HC}O_2 \rightarrow 3CO_2 + \frac{x}{2}H_2O \tag{21}$$

where: $\nu_{O2,HC}$ – an effective oxygen demand based on the propane/propylene mixing ratio.

An effective oxygen demand $\nu_{O2,HC}$ is defined as the mole-weighted average of the stoichiometric O_2 needs of

the two ingredients (propane and propylene) under complete oxidation:

$$C_3H_8 + 5O_2 \rightarrow 3CO_2 + 4H_2O \quad (22)$$

$$C_3H_6 + 4.5O_2 \rightarrow 3CO_2 + 3H_2O \quad (23)$$

Then, an effective oxygen demand comes from the lump composition weights:

$$\nu_{O2,HC} = \frac{5y_{C_3H_8} + 4.5y_{C_3H_6}}{y_{C_3H_8} + y_{C_3H_6}} \quad (24)$$

For any global reaction j (e.g., CO oxidation, NO reduction by CO, HC oxidation), the Arrhenius rate constant is equal [4, 9]:

$$k_{p,j}(T) = A_j \exp\left(-\frac{E_j}{RT}\right) \quad (25)$$

where: A_j – the pre-exponential factor (units consistent with orders), E_j – the activation energy, J·mol^{-1}, R – universal gas constant (8.314), J·mol^{-1}·K^{-1},

Table 2 presents the kinetic parameters used for each global reaction in the 1D catalyst model.

Table 2. Kinetic parameters for the 1D TWC model with reactions

CO oxidation	
A [1/s]	2.0×10^{14}
E [J/mol]	1.50×10^{5}
NO reduction	
A [1/s]	1.0×10^{11}
E [J/mol]	7.8×10^{4}
HC oxidation	
A [1/s]	1.5×10^{13}
E [J/mol]	1.04×10^{5}
Reaction orders	
CO	1.0
NO	1.0
HC	1.0
O_2	0.5 for CO oxidation
O_2	1.0 for HC oxidation

The kinetic constants (on a pressure basis) had to be converted ($k_p \rightarrow k_c$) into concentrations:

$$k_{c,j}(T) = k_{p,j}(T)\left(\frac{RT}{p_{unit}}\right)^{\Sigma_i \alpha_{ij}} \quad (26)$$

where: $k_{c,j}$ – is the effective volumetric kinetic constant (units depend on total reaction order), p_{unit} – is a reference pressure (10^5 Pa), (RT/p_{unit}) – the multiplier transfers the law from pressures to concentrations, maintaining the correct units, α_{ij} – empirical reaction order of species i in reaction j (can differ from stoichiometric coefficient).

A nondimensional temperature damper $f_j(T)$ was introduced to mitigate unrealistically high reaction rates predicted by global kinetics at elevated gas temperatures. Above the light-off region, effects such as oxygen-storage saturation, external or internal mass-transfer limits, and thermal aging reduce the effective activity of a TWC, which simple Arrhenius power-law models do not capture. The damper leaves kinetics unchanged in the mid-temperature regime but smoothly dampens rates in the high-temperature tail, preventing overshoot of conversion. This empirical high-T correction enables agreement with GT-SUITE references while preserving the model's simplicity and numerical robustness.

$$f_j(T) = \frac{1}{1 + \left(\frac{T}{T_{drop,j}}\right)^{n_j}} \quad (27)$$

where: $f_j(T)$ – the damper is dimensionless and limited between 0 and 1, n_j – steepness exponent (dimensionless), $T_{drop,j}$ – characteristic drop temperature, K. $T_{drop,j}$ and n_j are calibrated values for each reaction.

Table 3 presents the parameters used for the high-temperature clamps for each reaction in the 1D TWC model.

Table 3. High-temperature clamps

CO oxidation	
T_{drop}	800
n	21
NO reduction	
T_{drop}	780
n	14.5
HC oxidation	
T_{drop}	730
n	13

Power-law rate expressions (reaction rate) for each reaction j can be written as:

$$r_j = k_{c,j}(T) \cdot f_j(T) \prod_i C_i^{\alpha_{ij}} \quad (28)$$

where: r_i – volumetric reaction rate (per gas volume), mol·m^{-3}·s^{-1}, C_i – gas-phase (molar) concentration of species i, mol·m^{-3}.

Hence, for the three global reactions, their reaction rates can be explicitly written:

$$r_{CO_{ox}} = k_{CO_{ox}} \cdot f_{CO}(T) \cdot C_{CO}^{a_{CO}} \cdot C_{O_2}^{b_{O_2}} \quad (29)$$

$$r_{NO_{re}} = k_{NO_{re}} \cdot f_{NO}(T) \cdot C_{CO}^{a_{CO,r}} \cdot C_{NO}^{b_{NO}} \quad (30)$$

$$r_{HC_{ox}} = k_{HC_{ox}} \cdot f_{HC}(T) \cdot C_{HC}^{a_{HC}} \cdot C_{NO}^{b_{O_2,HC}} \quad (31)$$

With an explicit Euler scheme, species concentrations are updated segment-by-segment using the power-law reaction rates:

$$C_{CO}^{k+1} = C_{CO}^{k} - \left(r_{CO_{ox}} + 2 \cdot r_{NO_{re}}\right)\Delta t \quad (32)$$

$$C_{O_2}^{k+1} = C_{O_2}^{k} - \left(0.5 \cdot r_{CO_{ox}} + \nu_{O2,HC} \cdot r_{HC_{ox}}\right)\Delta t \quad (33)$$

$$C_{CO_2}^{k+1} = C_{CO_2}^{k} + \left(r_{CO_{ox}} + 2 \cdot r_{NO_{re}} + 3 \cdot r_{HC_{ox}}\right)\Delta t \quad (34)$$

$$C_{NO}^{k+1} = C_{NO}^{k} - 2 \cdot r_{NO_{re}} \cdot \Delta t \quad (35)$$

$$C_{HC}^{k+1} = C_{HC}^{k} - r_{HC_{ox}} \cdot \Delta t \tag{36}$$

At the reactor exit, outlet mole fractions y_i^{out} are obtained from the updated concentrations and the total molar concentration C_t:

$$y_i^{out} = \frac{C_i^{out}}{C_t} \tag{37}$$

$$C_t = \sum_i C_i^{out} \tag{38}$$

Component conversions are reported from inlet to outlet on a molar basis:

$$conv_i = 100\frac{y_i^{in} - y_i^{out}}{y_i^{in}}[\%] \tag{39}$$

Table 4 presents the input data used for simulating chemical reactions with the 1D catalyst model, together with its geometric parameters.

Table 4. Input data for the 1D TWC model with reactions

Simulation time [s]	2000
Temperature [K]	linear ramp (350 → 900)
Mass flow rate [kg/s]	0.02
Working medium and mole fraction [-]	
CO_2	0.147
H_2O	0.1
O_2	0.005228
H_2	0.001978
CO	0.006865
C_3H_8	0.000102
C_3H_6	0.000406
NO	0.003042
NO_2	0.00001
N_2	0.735369
sum	1
Tested catalyst	
Diameter [m]	0.1057 (4.16 in)
Length [m]	0.1501 (5.91 in)
Channel density [m^{-2}]	9.3×10^5 (600 cpsi)
Wall thickness [m]	1.09×10^{-4} (0.109 mm)
Active layer (washcoat)	Yes

2.3. NEDC emission test for 1D model validation

This section describes the extension of the developed 1D model and its application to the simulation of the New European Driving Cycle emission test, a standardized procedure used to assess vehicle emissions under controlled conditions. This allows for a direct comparison of the model's predicted pollutant reductions with established emission limits, thereby validating its accuracy and utility as a design tool. The model is validated by comparing predicted conversion efficiencies and temperature profiles to experimental data from real NEDC tests on vehicles [13]. This validation builds confidence in the model's accuracy for forecasting how three-way catalysts respond to changing real-world driving conditions, which is a key factor in effective emission control. This method enables detailed analysis of catalyst performance and optimization, without the excessive computational demands of higher-dimensional models [4, 12].

As an initial step in extending the model, the volumetric exhaust flow $\dot{V}_{TP}$ was obtained at the tail-pipe over the full NEDC. To interface it with the existing 1D catalyst model, it was converted to an equivalent inlet mass flow $\dot{m}$ using the ideal-gas density of the inlet mixture.

$$\dot{m}(t) = \dot{V}_{TP}(t) \cdot \rho_{in}(t) \tag{40}$$

$$\rho_{in}(t) = \frac{p_{in}(t) \cdot M_{mix}(t)}{RT_{in}(t)} \tag{41}$$

$$M_{mix}(t) = \sum_i y_i(t) \cdot M_i \tag{42}$$

where: $\dot{V}_{TP}$ – tail-pipe volumetric flow, m^3/s, ρ_{in} – mixture density at the catalyst inlet, kg/m^3, p_{in} – inlet pressure, Pa, M_{mix} – mean molar mass, kg/mol, R – universal gas constant (8.314), $J \cdot mol^{-1} \cdot K^{-1}$, T_{in} – inlet temperature, K, y_i – inlet mole fraction of species i, M_i – molar mass of species i, kg/mol, for example $M_{CO} = 28.0101$ kg/mol.

Test data outputs from NEDC test were provided as raw exhaust composition in vol% and ppm. For use in the 1D reactor, these inputs were converted to consistent mole fractions:

$$y_i = \frac{C_i[\%]}{100} \tag{43}$$

$$y_i = \frac{C_i[ppm]}{10^6} \tag{44}$$

A dedicated muffler block was added to account for downstream backpressure at the catalyst inlet. The muffler loss was represented by a power-law fit calibrated at idle:

$$\Delta p_{muf}(\dot{m}) = \Delta p_{idle}\left(\frac{\dot{m}}{\dot{m}_{idle}}\right)^n \tag{45}$$

where: Δp_{idle} – idle backpressure, Pa, $\dot{m}_{idle}$ – idle mass flow, kg/s, n – fit exponent (set to value 2).

The absolute pressure applied at the TWC inlet was the sum of ambient pressure and both drops (from TWC and muffler):

$$p_{in,TWC} = p_{atm} + \Delta p_{muf} + \Delta p_{TWC} \tag{46}$$

At idle ($\dot{m} \approx 0.003$ kg/s), the measured total backpressure upstream of the catalyst was $p_{in,TWC} \approx 24{,}000$ Pa, and the model parameters were calibrated to reproduce this point.

The emissions post-processor was implemented as a Simulink block (TWC_emissions) that converts mole to mass fractions, forms instantaneous mass rates, integrates cumulative masses, and reports g/km (or mg/km) over NEDC. The block operated at a fixed sample time (T_s = 1 s) and used the cycle distance $L_{cyc} = 11$ km.

From outlet (and inlet) mole fractions y_i and species molar masses M_i, the mixture molar mass M_{mix}, and mass fractions w_i were computed as:

$$w_i = \frac{y_i M_i}{M_{mix}} \quad (47)$$

Instantaneous mass rates (in/out) of species i, were computed as:

$$\dot{m}_i(t) = \dot{m}(t) \cdot w_i(t) \cdot 10^3 \ [g/s] \quad (48)$$

where: $\dot{m}$ – total mass flow rate, $kg \cdot s^{-1}$.

Cumulative masses M_i in [g] of species i for pre-TWC and post-TWC were determined by the trapezoidal integration:

$$M_i[k] = M_i[k-1] + \frac{1}{2}(\dot{m}_i[k-1] + \dot{m}_i[k])T_s \quad (49)$$

where: T_s – fixed sample time (1 s).

Tailpipe (post-TWC) emission index E_i of species i at the end of the cycle was reported as:

$$E_i = \frac{M_{i,out}(t_{end})}{L_{cyc}} \cdot 10^3 \ [mg/km] \quad (50)$$

where: L_{cyc} – the cycle distance (11 km).

For the NEDC simulation, the Arrhenius parameters were updated for each global reaction. Specifically, the pre-exponential factor and activation energy were calibrated to align the model's tailpipe CO/NO_x/HC with the measured NEDC g/km totals. The temperature high-T correction introduced earlier was retained to avoid unrealistic over-conversion at very high temperatures, ensuring stable fits across the full cycle.

Table 5 presents the calibrated kinetic parameters used for each global reaction of the 1D catalyst model in the NEDC emission cycle.

Table 5. Adjusted kinetic parameters for the 1D TWC model in NEDC test

CO oxidation	
A [1/s]	3.36×10^{16}
E [J/mol]	1.42×10^{5}
NO reduction	
A [1/s]	5.8×10^{11}
E [J/mol]	7.8×10^{4}
HC oxidation	
A [1/s]	2.25×10^{14}
E [J/mol]	1.04×10^{5}

Table 6. Input data for the 1D TWC model in the NEDC cycle

Simulation time [s]	1180
Temperature [K]	up to 927
Mass flow rate [kg/s]	up to 0.042
Working medium	exhaust gases
Tested catalyst	
Diameter [m]	0.1184 (4.66 in)
Length [m]	0.0762 (3.0 in)
Channel density [m^{-2}]	6.2×10^5 (400 cpsi)
Wall thickness [m]	1.65×10^{-4} (0.165 mm)
Active layer (washcoat)	Yes

Table 6 presents the input data used for simulating the NEDC emission cycle with the 1D catalyst model, together with its geometric parameters.

Figure 2 shows the NEDC cycle profile, which was conducted on a chassis dynamometer at the BOSMAL laboratory (Fig. 5).

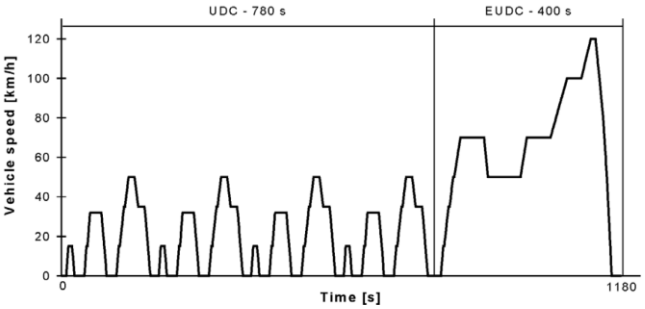

Fig. 2. Profile of the New European Driving Cycle [2]

Figure 3 shows the tested vehicle, a 2014 VW Golf VI 1.4 TSI (90 kW, Euro 5b). Figure 4 further presents the catalyst with the exhaust sampling probe and a thermocouple measuring temperature upstream of the catalytic reactor.

Fig. 3. Test vehicle evaluated under the NEDC driving cycle on a chassis dynamometer

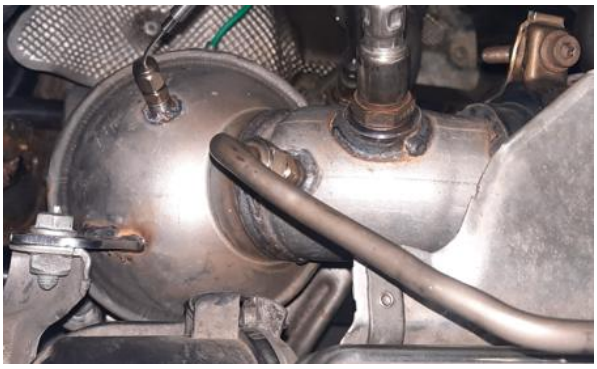

Fig. 4. Connections for raw exhaust gas sampling and temperature measurement upstream of the TWC catalyst

3. Modeling results

3.1. Pressure drop model and validation

A one-dimensional pressure-drop model of the TWC catalyst was implemented in MATLAB/Simulink. The inlet boundary conditions consisted of a ramped mass-flow rate and a fixed gas temperature, while constant geometric parameters (monolith diameter/length, cell density, wall thickness, washcoat used and absolute inlet pressure) were supplied as entrance blocks. The functional block (Fig. 6)

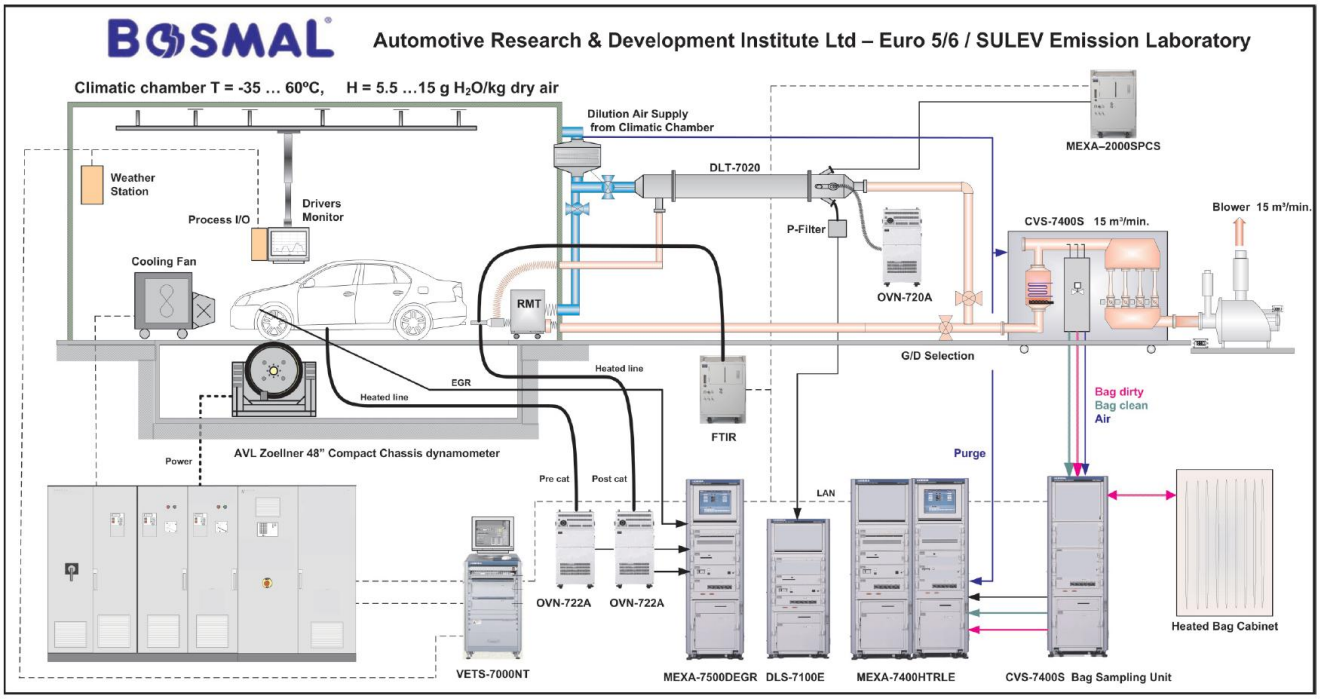

Fig. 5. Layout of the emission testing laboratory including climatic chamber, chassis dynamometer, dilution tunnel, and exhaust analysis system [3]

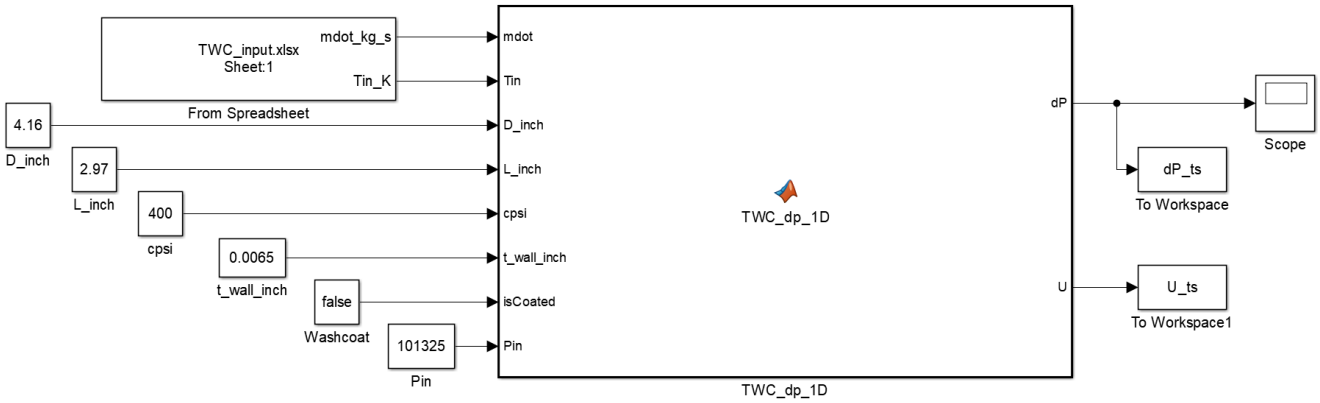

Fig. 6. One-dimensional pressure drop model for the three-way catalyst implemented in MATLAB/Simulink

was equipped with the code for the governing equations summarized in Section 2.1 (channel cross-section and OFA, ideal-gas density and viscosity model, average channel velocity, and viscous/inertial loss terms).

At the outputs, the total pressure drop across the catalyst and the corresponding mean channel velocity were computed. A post-processing script then compared the 1D model predictions with experimental measurements, reporting pressure-drop and channel-velocity agreement (Fig. 7). The model results show good agreement with literature (experimental) data reported by Ekström et al. [5], which were used for validation of the pressure-drop model.

To quantify the agreement between the 1D pressure-drop model and experimental data, the mean absolute percentage error (MAPE) was used. Lower MAPE indicates better agreement (0% is perfect).

$$\mathrm{MAPE}[\%] = \frac{100}{n}\sum_{i=1}^{n}\left|\frac{y_i^{exp} - y_i^{sim}}{y_i^{exp}}\right| \qquad (51)$$

where: y_i^{exp} – is the measured pressure drop at sample i, Pa, y_i^{sim} – is the simulated value for pressure drop at sample i, Pa, n – is the number of samples.

3.2. Reaction kinetics model and validation

An emission-chemistry model was implemented around a new 1D reaction block in MATLAB/Simulink. Exhaust-gas compositions (mole fractions, inlet temperature and flow) were first prepared in an Excel file and linked to the model via a From Spreadsheet source. The reaction block (Fig. 8) implements the power-law Arrhenius scheme summarized in Section 2.2 (global CO oxidation, NO reduction with CO, and HC oxidation), including the residence-time marching along the monolith.

For each time step the block advances species concentrations along the axial segments and computes outlet mole fractions and instantaneous conversions – these signals are logged to the MATLAB base workspace via To Workspace sinks.

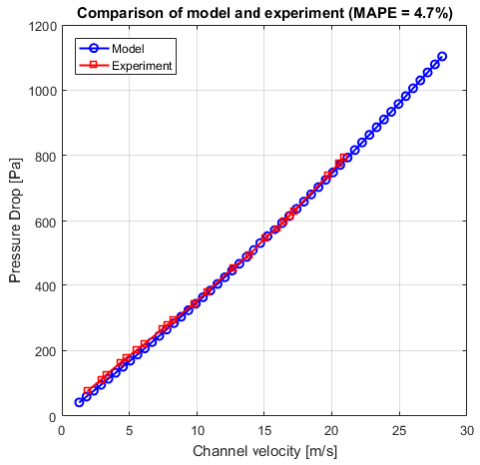

Fig. 7. Comparison of pressure drop across the TWC between the 1D model and experimental data

Validation focused on conversion versus time profiles for CO, NO, and HC. The GT-SUITE reference (from Excel file) and Simulink outputs were processed by a MATLAB script, which synchronized their time vectors and produced combined traces for all species. Across all three pollutants, the T50 (50% conversion) points from the 1D model and GT-SUITE intersected at the correct time, demonstrating strong agreement between the simulations. The initial baselines remained near zero and the final levels approached similar high conversion levels, giving satisfactory agreement at both the start and end of the transients. Figures 9–11 present representative plots, highlighting comparable rise slopes, T50 alignment, and asymptotic behavior.

The reaction kinetics model was calibrated through comparison with GT-POWER reference simulations. Arrhenius parameters and high-temperature reaction clamps were iteratively adjusted to match the transient conversion

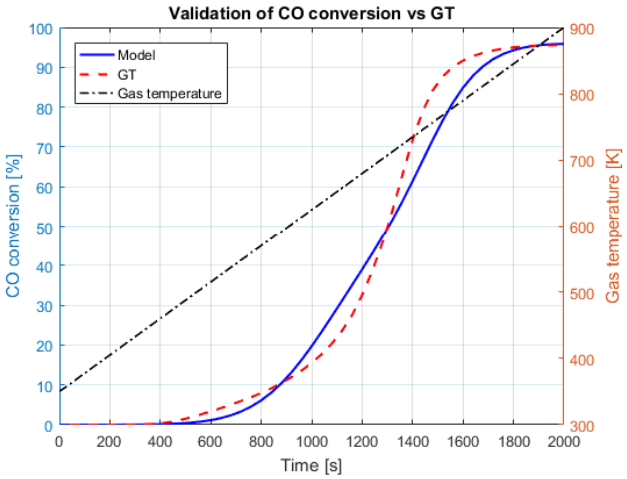

Fig. 9. Validation of CO conversion for the 1D catalyst model against GT simulation results

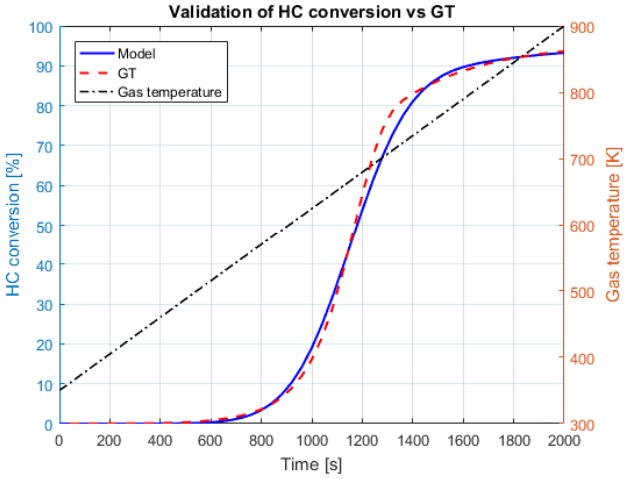

Fig. 10. Validation of HC conversion for the 1D catalyst model against GT simulation results

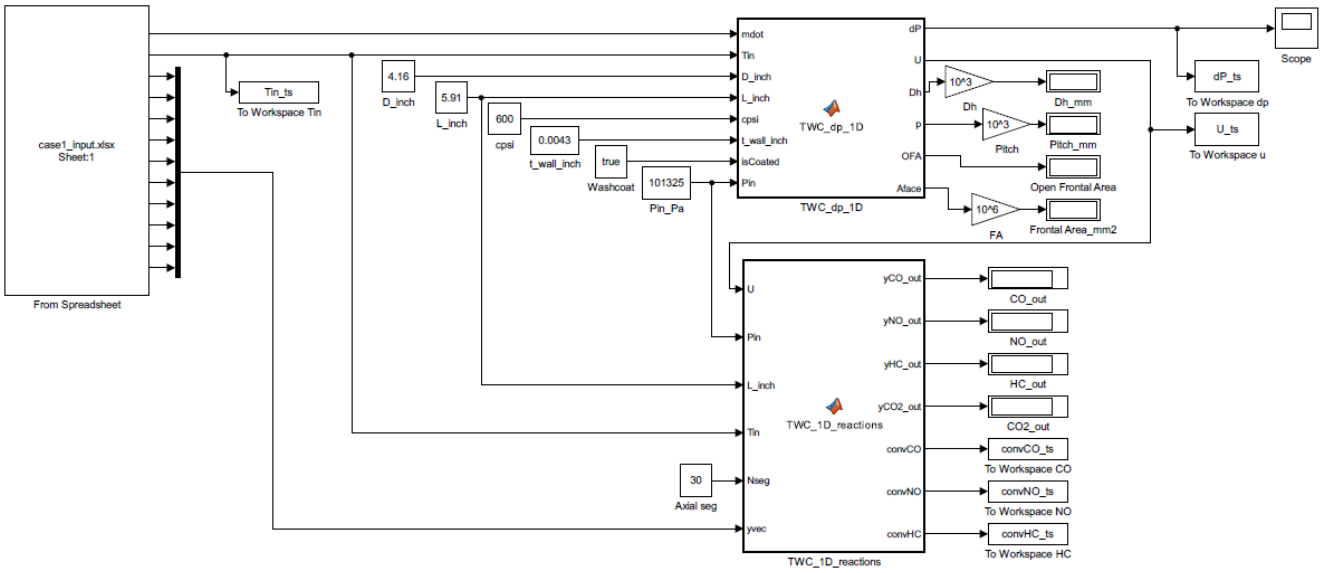

Fig. 8. One-dimensional reaction kinetics model for the three-way catalyst implemented in MATLAB/Simulink

profiles of CO, HC, and NO. Validation focused on the alignment of characteristic light-off behavior, including T10, T50, and T90 conversion points, as well as the overall shape of the conversion curves. The final parameter sets providing the best agreement are summarized in Tables 2 and 3.

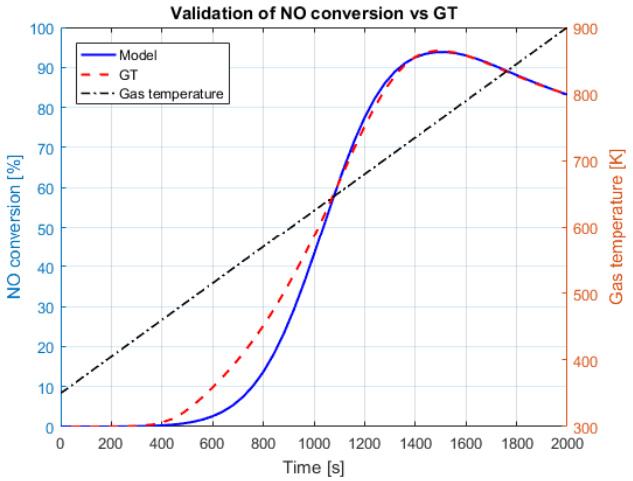

Fig. 11. Validation of NO conversion for the 1D catalyst model against GT simulation results

3.3. 1D model simulation in the NEDC test

The NEDC boundary conditions were assembled in an Excel file (time-resolved exhaust composition and temperature), then fed to the reaction block via From Spreadsheet in Simulink, analogously to the GT reference case. This provided the model with the full, second-by-second inlet vector over the ~1180 s cycle.

To reflect real exhaust system backpressure, a dedicated muffler pressure-drop block was added and calibrated to idle measurements. Its output was summed with ambient pressure to form the effective catalyst inlet pressure.

In addition, a "TWC_emissions" block (Fig. 12) was introduced to compute instantaneous tailpipe mass rates and cycle-cumulative emissions (pre- and post-TWC) for CO, NO_x, and HC, as well as final emission values (g/km) calculated for the NEDC cycle.

All computations in these functional blocks follow the formulations summarized in Section 2.3, providing a coherent assessment throughout the NEDC cycle of transient responses and cumulative emission outcomes.

A separate MATLAB script was used to generate the NEDC plots (Fig. 13–15). For each pollutant (CO, NO_x, HC) it produces two panels: instantaneous mass rate upstream and downstream of the TWC, and cumulative emissions pre- and post-TWC normalized to g/km. The cumulative panels include a black dashed line marking the corresponding EURO limit, which enables a direct visual check of compliance over the full cycle.

For the NEDC simulation, no vehicle or engine submodel was employed. Instead, the catalyst model was driven by measured, time-resolved exhaust gas composition, temperature, and mass flow obtained from the NEDC test,

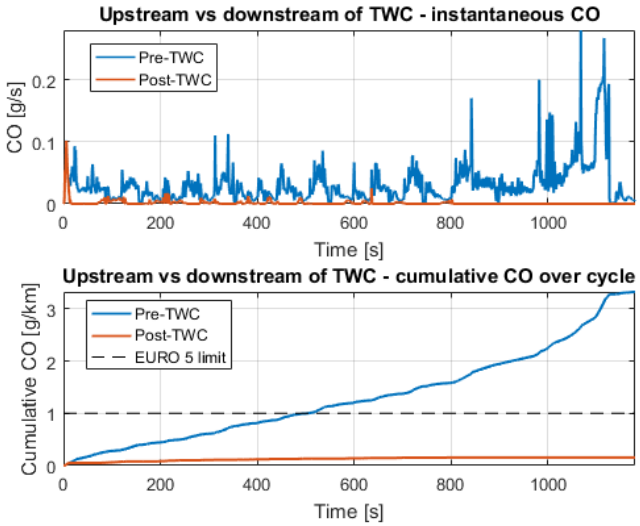

Fig. 13. Instantaneous and cumulative CO emissions upstream and downstream of the TWC from the 1D model during the NEDC cycle

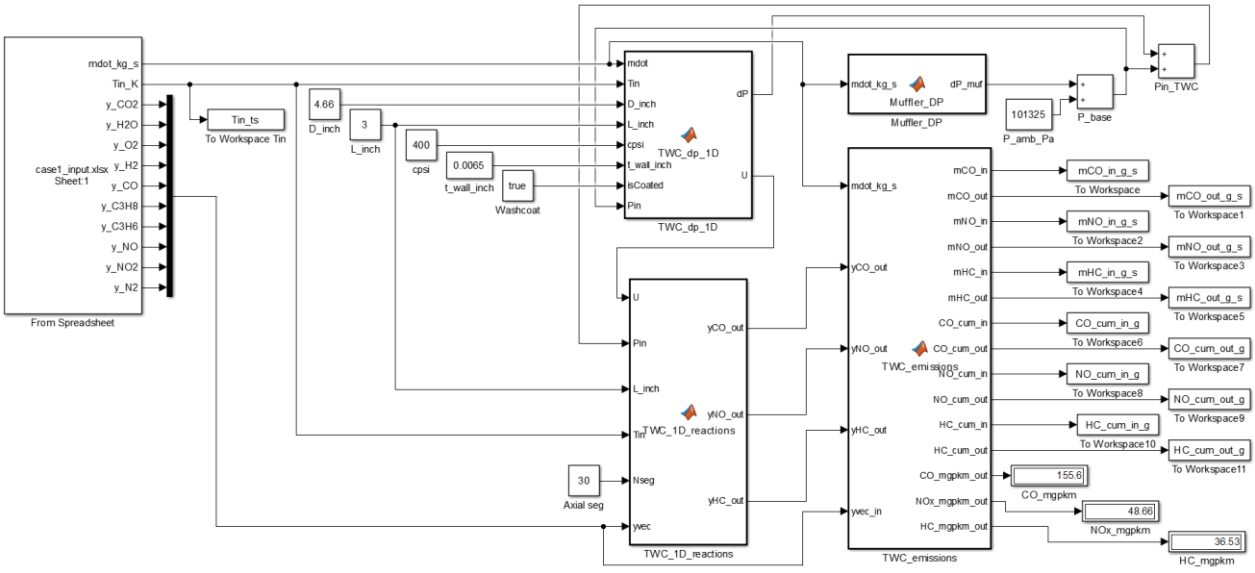

Fig. 12. One-dimensional model of the three-way catalyst under the NEDC driving cycle implemented in MATLAB/Simulink

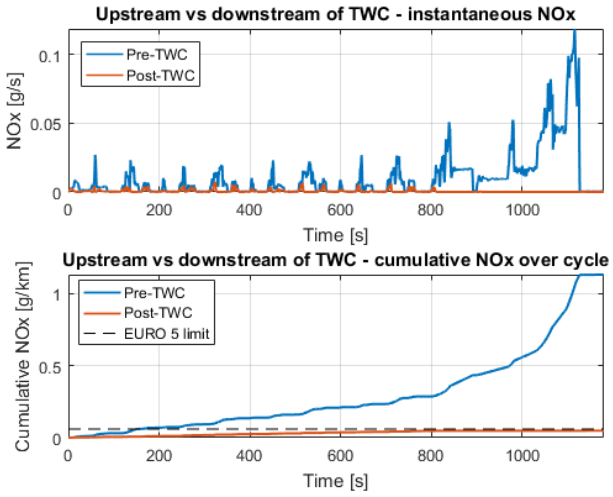

Fig. 14. Instantaneous and cumulative NO_x emissions upstream and downstream of the TWC from the 1D model during the NEDC cycle

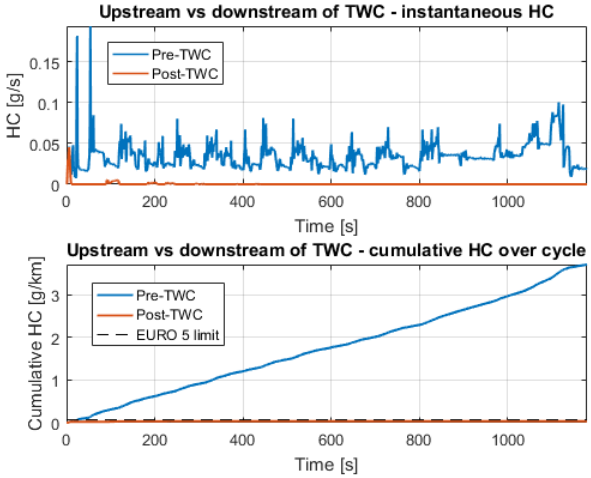

Fig. 15. Instantaneous and cumulative HC emissions upstream and downstream of the TWC from the 1D model during the NEDC cycle

which were applied directly as inlet boundary conditions. Since a different catalyst was used in the NEDC experiment, the kinetic parameters were recalibrated for this case, as summarized in Table 5.

Figures 13–15 illustrate instantaneous and cumulative emissions of CO, NO_x, and HC upstream and downstream of the TWC during the NEDC cycle. The post-TWC results show a substantial reduction of instantaneous emission peaks and cumulative tailpipe emissions compared to the pre-TWC signals. For all three pollutants, the cumulative emissions remain below the Euro 5 limits, confirming effective catalyst operation under experimentally measured NEDC conditions.

4. Summary and conclusion

This work presented a lightweight 1D plug-flow model of a three-way catalyst (TWC) in MATLAB/Simulink, expanded with a muffler backpressure block and an emissions post-processor. The model reproduces pressure-drop behavior, CO/NO_x/HC conversion trajectories, and cumulative tailpipe indices (g/km) over NEDC with satisfactory agreement against GT-SUITE and literature references, including consistent T50 light-off temperature and T10/T90 benchmarks. The model executes quickly, making it suitable for iterative calibration and sensitivity studies.

Calibration of Arrhenius parameters (A, E) proved stable and repeatable across operating profiles. Intentional simplifications, including 1D plug–flow, isothermal gas-phase, reduced chemistry (HC and NO_x lumped), and a high–temperature empirical damper, produced reliable trends and magnitudes while maintaining low model complexity. Including the muffler pressure–drop block enabled the inlet boundary pressure to capture realistic backpressure, enhancing agreement while preserving computational speed.

The present model neglects radial distributions and axial dispersion, is isothermal (no energy balance), and assumes no convective cooling, pore diffusion, or gas-film mass transfer. Kinetics follow fixed-order power-law forms without adsorption or coverage effects (no Langmuir-Hinshelwood), oxygen storage capacity (OSC), or side reactions or intermediates, while the high-T clamp is empirical. Calibrated A/E and temperature limits are case-dependent, so extending them beyond the validated range requires caution. Cold start conditions, reaction exotherms and hot-spots, as well as catalyst aging, are excluded from the model.

The integration of an energy balance, Langmuir–Hinshelwood coverage kinetics, and OSC dynamics should expand the model's scope and improve its predictive reliability, especially in light-off and high-load regimes. This approach can be applied to other aftertreatment devices (DPF/GPF, SCR) and linked with a simple engine model to enable full drive-cycle analysis. Advanced 3D CFD software, for example, ANSYS Fluent, can be used to verify geometric effects and provide input for reduced models. Overall, the proposed 1D model offers a practical balance between accuracy and speed for evaluating designs, calibrating kinetics, and assessing emission-reduction performance over regulatory cycles.

The main contribution of this work is the development of an original one-dimensional three-way catalyst model built from scratch in MATLAB/Simulink, a platform that does not provide a ready-made aftertreatment or catalyst module. The proposed model enables prediction of catalyst pressure drop, pollutant conversion efficiency, and tailpipe emissions over the NEDC cycle using a unified and computationally efficient framework. Owing to its modular structure, the model can be easily adapted to different catalyst geometries and recalibrated for various kinetic parameter sets. Furthermore, the developed approach provides a flexible foundation for future extensions toward more advanced exhaust aftertreatment configurations and integrated drive-cycle simulations.

Acknowledgements

The author of this article expresses gratitude to DRiV for funding the research. Additional appreciation is extended to the State University of Applied Sciences in Racibórz for supporting participation in the IX Young Scientists Academy conference and for funding the publication of this article.

Nomenclature

MAPE mean absolute percentage error
NEDC New European Driving Cycle
OSC oxygen-storage capacity
TWC three-way catalyst

Bibliography

[1] Aslanjan J, Klauer C, Perlman C, Günther V, Mauß F. Simulation of a three-way catalyst using transient single and multi-channel models. SAE Technical Paper 2017-01-0966. 2017. https://doi.org/10.4271/2017-01-0966

[2] Bielaczyc P, Szczotka A. The potential of current european light duty CNG-fuelled vehicles to meet Euro 6 requirements. Combustion Engines. 2012;151(4):20-33. https://doi.org/10.19206/ce-117018

[3] Bielaczyc P, Szczotka A, Pajdowski P, Woodburn J. Development of automotive emissions testing equipment and test methods in response to legislative, technical and commercial requirements. Combustion Engines. 2013;152(1):28-41. https://doi.org/10.19206/ce-117010

[4] Depcik C, Assanis D. One-dimensional automotive catalyst modeling. Prog Energy Combust Sci. 2005;31(4):308-369. https://doi.org/10.1016/j.pecs.2005.08.001

[5] Ekström F, Andersson B. Pressure drop of monolithic catalytic converters experiments and modeling. SAE Technical Paper 2002-01-1010. 2002. https://doi.org/10.4271/2002-01-1010

[6] Hayes RE, Mukadi LS, Votsmeier M, Gieshoff J. Three-way catalytic converter modelling with detailed kinetics and washcoat diffusion. Top Catal. 2004;30:411-415. https://doi.org/10.1023/b:toca.0000029783.16199.f3

[7] Holder R, Bollig M, Anderson DR, Hochmuth JK. A discussion on transport phenomena and three-way kinetics of monolithic converters. Chem Eng Sci. 2006;61(24):8010-8027. https://doi.org/10.1016/j.ces.2006.09.030

[8] Kakoee A, Hunicz J, Mikulski M. Integrated 1D simulation of aftertreatment system and chemistry-based multizone RCCI combustion for optimal performance with methane oxidation catalyst. J Mar Sci Eng. 2024;12(4):594. https://doi.org/10.3390/jmse12040594

[9] Koltsakis GC, Stamatelos AM. Modeling dynamic phenomena in 3-way catalytic converters. Chem Eng Sci. 1999; 54(20):4567-4578. https://doi.org/10.1016/s0009-2509(99)00130-x

[10] Kurzydym D, Klimanek A, Żmudka Z. Experimental and numerical analysis of flow through catalytic converters for original part and WALKER's replacement using reverse engineering and CFD. IOP Conf Ser Mater Sci Eng. 2018; 421(4):042044. https://doi.org/10.1088/1757-899x/421/4/042044

[11] Kuta K, Nadimi E, Przybyła G, Żmudka Z, Adamczyk W. Ammonia CI engine aftertreatment systems design and flow simulation. Combustion Engines. 2022;190(3):3-10. https://doi.org/10.19206/ce-143158

[12] Maio DD, Beatrice C, Fraioli V, Napolitano P, Golini S, Rutigliano FG. Modeling of three-way catalyst dynamics for a compressed natural gas engine during lean–rich transitions. Appl Sci. 2019;9(21):4610. https://doi.org/10.3390/app9214610

[13] Montenegro G, Onorati A. 1D thermo-fluid dynamic modeling of reacting flows inside three-way catalytic converters. SAE Int J Engines. 2009;2(1):14441459. https://doi.org/10.4271/2009-01-1510

[14] Papadopoulos C, Kourtelesis M, Dimaratos A, Moschovi AM, Yakoumis I, Samaras Z. Mechanistic aspects of the chemical reactions in a three-way catalytic converter containing Cu and platinum group metals. Processes. 2025; 13(3):649. https://doi.org/10.3390/pr13030649

[15] Pontikakis GN, Konstantas GS, Stamatelos AM. Three-way catalytic converter modeling as a modern engineering design tool. J Eng Gas Turbines Power. 2004;126(4):906-923. https://doi.org/10.1115/1.1787506

[16] Ramanathan K, Sharma CS. Kinetic parameters estimation for three way catalyst modeling. Ind Eng Chem Res. 2011; 50(17):9960-9979. https://doi.org/10.1021/ie200726j

[17] Real M, Hedinger R, Pla B, Onder C. Modelling three-way catalytic converter oriented to engine cold-start conditions. Int J Engine Res. 2019;22(2):640-651. https://doi.org/10.1177/1468087419853145

[18] Watling TC, Cox JP. Factors affecting three-way catalyst light-off: a simulation study. SAE Int J Engines. 2014;7(3): 1311-1325. https://doi.org/10.4271/2014-01-1564

[19] Wurzenberger JC, Peters B. Catalytic converters in a 1D cycle simulation code considering 3D behavior. SAE Technical Paper. 2003-01-1002. 2003. https://doi.org/10.4271/2003-01-1002

[20] Zhu Z, Midlam-Mohler S, Canova M. Development of physics-based three-way catalytic converter model for real-time distributed temperature prediction using proper orthogonal decomposition and collocation. Int J Engine Res. 2019; 22(3):873-889. https://doi.org/10.1177/1468087419876127

Damian Kurzydym, DEng. – Institute of Technology, University of Applied Sciences in Racibórz; Aftremarket Emission Control Engineering, DRiV Poland Sp. z o.o. (Tenneco division), Poland.
e-mail: *damian.kurzydym@akademiarac.edu.pl*